Published in final edited form as:
AJR Am J Roentgenol. 2014 December ; 203(6): W605–W613. doi:10.2214/AJR.14.12644.

Diagnostic Performance of Dual-Energy CT Stress Myocardial Perfusion Imaging: Direct Comparison With Cardiovascular MRI

Sung Min Ko[1], **Meong Gun Song**[2], **Hyun Kun Chee**[2], **Hweung Kon Hwang**[3], **Gudrun Maria Feuchtner**[4], and **James K. Min**[5]

[1]Department of Radiology, Konkuk University Medical Center, Konkuk University School of Medicine, 120-1 Neungdong-ro, Hwayang-dong, Gwangjin-gu, Seoul, 143-729, Korea

[2]Department of Thoracic Surgery, Konkuk University Medical Center, Konkuk University School of Medicine, Seoul, Korea

[3]Department of Cardiology; Konkuk University Medical Center, Konkuk University School of Medicine, Seoul, Korea

[4]Department of Radiology II, Innsbruck Medical University, Innsbruck, Austria

[5]Institute for Cardiovascular Imaging, Weill Cornell Medical College and the New York Presbyterian Hospital, New York, NY

Abstract

OBJECTIVE—The purpose of this study was to assess the diagnostic performance of stress perfusion dual-energy CT (DECT) and its incremental value when used with coronary CT angiography (CTA) for identifying hemodynamically significant coronary artery disease.

SUBJECTS AND METHODS—One hundred patients with suspected or known coronary artery disease without chronic myocardial infarction detected with coronary CTA underwent stress perfusion DECT, stress cardiovascular perfusion MRI, and invasive coronary angiography (ICA). Stress perfusion DECT and cardiovascular stress perfusion MR images were used for detecting perfusion defects. Coronary CTA and ICA were evaluated in the detection of ≥ 50% coronary stenosis. The diagnostic performance of coronary CTA for detecting hemodynamically significant stenosis was assessed before and after stress perfusion DECT on a pervessel basis with ICA and cardiovascular stress perfusion MRI as the reference standard.

RESULTS—The performance of stress perfusion DECT compared with cardiovascular stress perfusion MRI on a per-vessel basis in the detection of perfusion defects was sensitivity, 89%; specificity, 74%; positive predictive value, 73%; negative predictive value, 90%. Per segment, these values were sensitivity, 76%; specificity, 80%; positive predictive value, 63%; and negative predictive value, 88%. Compared with ICA and cardiovascular stress perfusion MRI per vessel territory the sensitivity, specificity, positive predictive value, and negative predictive value of coronary CTA were 95%, 61%, 61%, and 95%. The values for stress perfusion DECT were 92%, 72%, 68%, and 94%. The values for coronary CTA and stress perfusion DECT were 88%, 79%,

Address correspondence to S. M. Ko (ksm9723@kuh.ac.kr).

73%, and 91%. The ROC AUC increased from 0.78 to 0.84 ($p = 0.02$) with the use of coronary CTA and stress perfusion DECT compared with coronary CTA alone.

CONCLUSION—Stress perfusion DECT plays a complementary role in enhancing the accuracy of coronary CTA for identifying hemodynamically significant coronary stenosis.

Keywords

cardiovascular MRI; coronary artery disease; CT; dual-energy CT; ischemia

Coronary CT angiography (CTA) enables noninvasive detection of anatomically high-grade coronary stenoses with high sensitivity and negative predictive value but is prone to false-positive findings stemming from overestimation of stenosis severity and artifacts, including calcification and motion [1, 2]. Furthermore, a coronary CTA finding of stenosis alone does not determine the hemodynamic significance of a coronary lesion [3, 4]. Therefore, there is great interest in combining coronary CTA with SPECT or cardiovascular stress perfusion MRI [5–7]. The proficiency of stress perfusion CT for the diagnosis of hemodynamically significant coronary artery disease (CAD) has been assessed against an array of reference standards, including SPECT, fractional flow reserve (FFR), and cardiovascular stress perfusion MRI, in several studies [8–15]. In those early studies, the addition of perfusion CT to coronary CTA improved diagnostic accuracy for discrimination of ischemia-causing coronary lesions [10–15].

Improvements in technology allow dual-energy CT (DECT) with image reconstruction of iodine maps. These maps are used to analyze iodine distribution within the myocardium on the basis of the specific absorption characteristics of iodine at different x-ray energies. Initial study results suggest that DECT images acquired at rest can depict reversible, stress-induced myocardial perfusion defects as seen on SPECT images and has the potential to more sensitively depict myocardial blood-pool defects than do single-energy CT spectra [16–18]. In small pilot studies [19, 20], stress perfusion DECT has had good diagnostic accuracy in the detection of stress-induced perfusion defects, as seen at cardiovascular stress perfusion MRI, and has played a complementary role in enhancing the diagnostic accuracy of coronary CTA for identifying significant coronary stenoses. To our knowledge, the diagnostic performance of stress perfusion DECT against an anatomic-physiologic reference standard has not been evaluated in a large population of consecutively enrolled patients with CAD. In addition, most perfusion CT studies have included myocardial segments with partial reversible ischemia and myocardial infarcts, which might have led to overoptimistic results of perfusion CT [8–15]. Accordingly, positive findings at perfusion CT may be identifying only segments with markedly severe CAD or chronic myocardial infarction. We evaluated the performance of stress perfusion DECT and its incremental value when used with coronary CTA for the detection and exclusion of hemodynamically significant coronary stenoses causing complete reversible perfusion defects compared with the combination of invasive coronary angiography (ICA) and cardiovascular stress perfusion MRI as the reference standard.

Subjects and Methods

Study Population and Design

The study protocol was approved by the institutional review board, and all patients gave written informed consent before enrollment. From May 2010 to May 2012, consecutively enrolled patients were evaluated according to the following inclusion criteria: age 40 years or older; hemodynamically significant coronary stenoses (≥ 50% luminal reduction) or inability to evaluate the coronary arteries owing to extensively calcified plaque, stent, or cardiac motion artifact detected with coronary CTA; and absence of evidence of chronic myocardial infarction at coronary CTA. We excluded patients with chronic myocardial infarction because this study was confined to myocardial ischemia alone. All participants were considered for nonurgent revascularization. Exclusion criteria were atrial fibrillation, impaired renal function (serum creatinine level > 1.5 mg/dL, glomerular filtration rate < 60 mL/min/1.73 m^2), severe asthma, contraindication to cardiovascular MRI (incompatible metallic implants, claustrophobia), previous coronary artery bypass graft surgery, previously known myocardial infarction, and unstable clinical status (including critical aortic stenosis and New York Heart Association class IV congestive heart failure). Enrolled patients underwent stress perfusion DECT, cardiovascular stress perfusion MRI, and ICA within 30 days without intervening change in clinical status or coronary revascularization.

Image Acquisition

Coronary CT angiography—All CT examinations were performed with a dual-source CT scanner (Somatom Definition, Siemens Healthcare) with the following scanning parameters: collimation, 32 × 0.6 mm; slice acquisition, 64 × 0.6 mm with *z*-flying focal spot technique; gantry rotation time, 330 milliseconds; pitch, 0.20–0.43 adapted to heart rate; tube voltage, 100 or 120 kV (depending on age and body mass index); and tube current–time product, 320 mAs/rotation. Before the helical scan, an unenhanced ECG-gated CT scan, prospectively triggered at 75% of the R-R interval, was obtained to measure the coronary calcium score. For coronary CTA, ECG-based tube current modulation was implemented with the MinDose protocol (Siemens Healthcare), except in patients with a mean heart rate more than 80 beats/min or with arrhythmia. The full dose window of 30–80% of the cardiac cycle was used for patients with heart rates of 65–79 beats/min; the full dose window of 60–80% of the cardiac cycle was used for patients with heart rates less than 65 beats/min. To detect areas of delayed enhancement, delayed contrast-enhanced imaging was performed 5 minutes later using a tube voltage of 100 kV; tube current–time product, 250 mAs/rotation; and prospective ECG-triggering covering 65% of the R-R interval.

Patients with a prescan heart rate greater than 65 beats/min were administered 50–100 mg of metoprolol orally 1 hour before coronary CTA. All patients received 0.6 mg of nitroglycerin sublingually immediately before coronary CTA. Contrast administration was controlled with a bolus-tracking technique. For all CT examinations, a dual-head power injector (Stellant D, Medrad) was used to administer a three-phase bolus at a rate of 4.5 mL/s. First, 70–80 mL of undiluted contrast medium (iopromide, Ultravist 370 mg I/mL, Bayer-Schering Pharma) was administered after optimal timing determination via a bolus-tracking technique. Forty-five

milliliters of a mixture of 70% contrast medium to 30% saline solution was administered, with a saline chaser, for coronary CTA.

Myocardial perfusion dual-energy CT—All patients were subsequently scanned on a separate day within 60 days of coronary CTA. Imaging was a stress-only DECT myocardial perfusion examination with no premedication with β-blockers or nitroglycerin. Stress perfusion DECT was performed in a single-phase acquisition with the same imaging parameters as for coronary CTA, as follows: One x-ray tube was operated with 82 mAs/rotation at 140 kV and the second tube with 164 mAs/rotation at 80 kV. Retrospectively ECG-gated imaging with tube current modulation and pitch adaptation was performed 4 minutes after initiation of adenosine administration at a constant rate of 140 μg/kg/min. Full tube current was applied from 60% to 75% of the cardiac cycle, and tube current reduction to 4% was applied outside the adjusted pulsing window. Image acquisition was started 9 seconds after the signal attenuation level reached the predefined threshold of 120 HU at the aortic root. Rest perfusion and delayed enhancement DECT were not performed because of previous acquisition by single-energy coronary CTA.

Cardiovascular myocardial perfusion MRI—Within 7 days after stress perfusion DECT, myocardial perfusion cardiovascular MRI examinations were performed with a 1.5-T system (Signa HDxt, GE Healthcare) with an eight-element phased-array surface coil or a 3-T system (Magnetom Skyra, Siemens Healthcare) with a 32-channel body coil. Perfusion data were acquired in three left ventricular short-axis slices (basal, midventricular, and apical) during a breath-hold in end-expiration. The adenosine administration protocol was identical to that for stress perfusion DECT. During adenosine infusion, an IV bolus of 0.1 mmol/kg gadopentetate dimeglumine (Magnevist, Bayer Schering Pharma) was injected; adenosine infusion was stopped after completion of the sequence. Ten minutes after first-pass myocardial perfusion imaging, rest perfusion imaging was performed with a second bolus of 0.1 mmol/kg gadopentetate dimeglumine. Perfusion data were acquired with the 1.5-T system by use of a hybrid of a gradient-echo and an echo-planar pulse sequence (TR/TE, 1.2/270; flip angle, 25°; slice thickness, 8 mm; preparation pulse, 90° for each slice; echo-train length, 4; FOV, 360 × 360 mm; matrix, 128 × 128; pixel size, 2.8 × 2.8 mm) or with the 3-T system by use of a turbo FLASH (TR/TE, 156/1.03; flip angle, 10°; slice thickness, 8 mm; saturation recovery time, 100 milliseconds; FOV, 360 × 274 mm; matrix, 192 × 142; pixel size, 1.9 × 1.9 mm). Ten minutes after administration of the second bolus, delayed enhancement images were acquired in two long axes and 10 or 11 short axes by use of the 1.5-T system with a phase-sensitive myocardial delayed enhancement sequence or the 3-T system with a phase-sensitive inversion recovery sequence. The inversion time was chosen individually according to a cine inversion recovery or an inversion time scout image to optimize myocardial nulling.

Invasive coronary angiography—ICA (Allura Xper FD-10 system, Philips Healthcare) was performed in direct accordance with societal guidelines and within 4 days after cardiovascular MRI. A minimum of six projections were obtained: four views of the left coronary artery and two of the right coronary artery.

Image Processing and Interpretation

Coronary CT angiography—Coronary CTA images were reconstructed with a slice thickness of 0.75 mm. The reconstruction increment was set at 0.4 mm with a medium soft-tissue convolution kernel (B26f). For postprocessing, the coronary CTA datasets at the cardiac phase with the highest image quality were evaluated at a dedicated 3D workstation (Vitrea 2, version 4, Vital Images). Coronary artery segments of the three main coronary arteries and their major side branches with a luminal diameter of 1.5 mm or larger were classified according to a modified 16-segment American Heart Association (AHA) coronary model previously described [21]. Lesions with ≥ 50% reduction in luminal diameter were considered significant. Coronary segments with extensively calcified plaque or a small stent lumen with dense stent material were considered significant lesions because determination of the exact degree of stenosis in the lesion was impossible owing to the blooming artifact. Coronary segments with severely blurred or doubled vessel contours related to cardiac motion artifacts were also considered nonevaluable. A coronary vessel was considered significantly stenosed if one or more segments were nonevaluable or had ≥ 50% or greater lumen reduction. CT image quality was determined with the following subjective 4-point ranking scale: 1, excellent; 2, good; 3, moderate; 4, poor. Short-axis multiplanar reformatted images were obtained with a 5-mm slice thickness and no intersection gap at the middiastolic phase for resting perfusion CT analysis. Coronary CTA images were evaluated by an experienced radiologist blinded to other imaging data and to clinical information.

Myocardial perfusion dual-energy CT—Datasets for myocardial perfusion evaluation were analyzed at a slice thickness of 0.75 mm and a slice increment of 0.4 mm with a dedicated dual-energy convolution kernel (D26f) in the middiastolic phase [16]. The DECT-based iodine distribution maps were superimposed onto gray-scale multiplanar reformats of the left ventricular myocardium in the short-axis views (5-mm slice thickness, no intersection gap) by use of the dual-energy image postprocessing software application (syngo-DualEnergy, Syngo-Multimodality Workplace, Siemens Healthcare). Iodine maps were set to narrow window width and level settings (width, 260 HU; level, 130 HU), but the reading radiologists were allowed to adjust settings as needed. Perfusion defects were assessed visually and defined as contiguous circumscribed areas of reduced or absent iodine content within the left ventricular myocardium relative to remote normal-appearing myocardium, as has been previously described [18]. The stress perfusion DECT and rest perfusion CT images obtained at coronary CTA were read side by side in the short-axis view to differentiate stress-induced perfusion defects from artifacts or myocardial infarction. Two different independent radiologists blinded to all patient and imaging data, including coronary CTA, ICA, and cardiovascular MRI findings, used the AHA 17-segment model and three vascular territorial distributions [22] to evaluate the DECT-based iodine maps for perfusion assessment. AHA segment 17, corresponding to the apex, was excluded from the analysis. A perfusion defect of two or more segments was considered positive for ischemia at both stress perfusion DECT and cardiovascular stress perfusion MRI.

Cardiovascular myocardial perfusion MRI—Cardiovascular perfusion MR images were reviewed at a 3D workstation (Advantage Windows, GE Healthcare, or Syngo, Siemens Healthcare). Myocardial perfusion was determined in the standard manner

previously described, which was similar to the method for stress perfusion DECT. The presence of hypoenhancement in a coronary artery territory persisting for more than six heartbeats under adenosine stress was considered positive for a perfusion defect [23]. Delayed enhancement images were analyzed visually for the detection of hyperenhanced segments from the subendocardium to the epicardium. All stress, rest, and delayed enhancement cardiovascular MR images were independently analyzed by two experienced radiologists blinded to all patient and the imaging data, including coronary CTA, ICA, and stress perfusion DECT findings.

Invasive coronary angiography—Quantitative assessment of stenosis severity percentage at ICA was performed with standard commercial software (CAAS, Pie Medical) by a cardiologist with 25 years' experience in coronary intervention. Coronary artery segments were defined as for coronary CTA: ≥ 50% stenosis was considered anatomically obstructive. A coronary vessel was considered significantly stenosed if at least one segment was nonevaluable or had ≥ 50% lumen reduction.

Matching of Perfusion Segments to Corresponding Vascular Territories

A blinded independent physician mapped coronary CTA vascular territories to myocardial segments for both DECT and cardiovascular perfusion MRI, as has been previously described [9, 11]. Vessel dominance was used to decide on the vessel supplying the inferior and inferoseptal territories. According to whether obtuse marginal or diagonal branches supplied the anterolateral wall, either the left circumflex or left anterior descending (LAD) vessel was defined as supplying the mid and basal anterolateral wall. The ramus intermedius was defined as supplying the anterior wall or anterolateral wall. The large septal perforator of the LAD was defined as supplying the inferior septum. In addition, the distal LAD wrapped around the apex was defined as supplying the apical inferior wall.

Hemodynamically significant coronary stenosis and reference standard—An angiographically significant stenotic (≥ 50% reduction in luminal diameter) or nonevaluable vessel was considered as causing or not causing ischemia if a perfusion defect was observed or not observed in the same vascular territory. A perfusion defect in a vascular territory subtended by a coronary vessel with < 50% stenosis was considered a false-positive result. Furthermore, the presence or absence of hemodynamically significant coronary stenosis per patient or per vascular territory was also combined through use of a combination of coronary CTA and stress perfusion DECT versus a combination of ICA and cardiovascular perfusion MRI. Per-vessel analyses included the LAD, left circumflex, and right coronary artery territories.

Radiation dose—The effective radiation dose for the coronary CTA (including calcium scoring, coronary CTA, and delayed enhancement) and stress perfusion DECT examination was calculated in all patients. The dose-length product was converted to millisieverts by multiplication of dose-length product by the conversion coefficient factor 0.014 $mSv \cdot mGy^{-1} \cdot cm^{-1}$ [24].

Statistical Analysis

Quantitative variables were expressed as mean ± SD, and categoric variables were expressed as frequencies or percentages. The McNemar test was used for comparison of paired proportions. Sensitivity, specificity, and positive and negative predictive values were calculated from 2 × 2 contingency tables and their respective 95% CIs from binomial expressions. ROC analysis was performed, and the AUC was calculated for all diagnostic testing strategies for which a reference standard was available. Kappa statistics were used for interobserver agreement and intermodality concordance. A value of $p < 0.05$ was considered statistically significant. Statistical analyses were performed with SAS software (version 9.1, SAS Institute). We also used PASS 2008 statistical software (NCSS) to perform a two-ROC-curve power analysis for validation of the study purpose or hypothesis.

Results

Patient Population

The study population consisted of 100 patients (67 men, 33 women; mean age, 62.7 ± 8.2 years; range, 40–78 years). The study population characteristics are shown in Table 1.

Coronary CT Angiographic and Stress Perfusion Dual-Energy CT Findings

The average heart rate at coronary CTA was 70 ± 15 beats/min, and the mean Likert score was 1.2 ± 0.4. The mean radiation exposure from calcium scanning was 0.74 ± 0.16 mSv; coronary CTA, 5.3 ± 1.6 mSv; and delayed enhancement scanning, 1.2 ± 0.2 mSv. Accordingly, mean radiation exposure for the coronary CTA protocol was 7.3 ± 1.7 mSv (range, 5.2–11.4 mSv). The median Agatston calcium score was 208 (interquartile range, 31.0–461.5). Eighty-one segments were considered nonevaluable because of extensively calcified plaque ($n = 73$) and the presence of a stent ($n = 8$). Stenosis ≥ 50% was identified in 282 (18%) segments and 183 (61%) vessels. On a per-patient basis, ≥ 50% stenosis was identified as one-vessel, two-vessel, and three-vessel CAD for 44%, 29%, and 27% of the population.

Stress perfusion DECT was completed for all patients within 20 ± 17 days of coronary CTA. The mean heart rate was 84 ± 17 beats/min at stress. The mean heart rate difference was 13 ± 14 beats/min. The mean image quality score was 1.7 ± 0.6 with an effective radiation dose of 4.2 ± 1.1 mSv (range, 2.6–7.3 mSv). Forty-seven (2.9%) myocardial segments were not evaluable because of cardiac motion artifact ($n = 30$) and beam-hardening artifact ($n = 17$). Perfusion defects were identified in 89 (89%) patients, 160 (53%) vascular territories, and 576 (37%) segments (Figs. 1–4). Among patients with perfusion defects, 41 (46%) had a defect involving one vessel territory; 27 (30%), two vessel territories; and 16 (18%), three vessel territories. Good interobserver agreement (87%) was found for identification of perfusion defects (per segment $\kappa = 0.73$).

Invasive Coronary Angiographic and Cardiovascular Stress Perfusion MRI Findings

The ICA findings showed that 82 (82%) patients had significant stenosis in at least one coronary vessel; 37 of these patients had significant stenosis in the right coronary artery territory, 70 in the LAD territory, and 37 in the left circumflex territory. Among those with

significant anatomic stenosis, 36 (44%) patients had one-vessel disease, 30 (37%) had two-vessel disease, and 16 (20%) had three-vessel disease.

Cardiovascular perfusion MRI was performed within 2.4 ± 0.8 days of perfusion DECT with the 1.5-T MRI system for 60 patients and the 3-T MRI system for 40 patients. All cardiovascular MR images were of diagnostic quality with an average Likert score of 1.3 ± 0.5. Reversible perfusion defects were identified in 75 (75%) patients, 130 (43%) vascular territories, and 490 (31%) myocardial segments (Figs. 1 and 2). Cardiovascular MRI showed perfusion defects in one vessel territory in 38 (51%) patients, two vessel territories in 19 (25%) patients, and three vessel territories in 18 (24%) patients. There was good interobserver agreement (93%) in identification of perfusion defects per segment ($\kappa = 0.84$).

Diagnostic Performance of Stress Perfusion Dual-Energy CT Versus Cardiovascular Perfusion MRI

Stress perfusion DECT depicted 576 segments with perfusion defects. Of these, 365 (63%) were detected with cardiovascular MRI (Figs. 1 and 2), and 211 (37%) were not (Fig. 3). One hundred fourteen (24%) segments with perfusion defects on cardiovascular MR images were not identified with stress perfusion DECT. The diagnostic performance of stress perfusion DECT compared with cardiovascular MRI per segment, per vascular territory, and per patient is shown in Table 2.

Diagnostic Performance of Coronary CT Angiography With Stress Perfusion Dual-Energy CT Versus Invasive Coronary Angiography With Cardiovascular Stress Perfusion MRI

Combined coronary CTA and stress perfusion DECT showed that 88 (88%) patients had 141 (47%) vessel territories subtended by hemodynamically significant coronary stenosis causing perfusion defects. This finding compared favorably to the combined ICA and cardiovascular stress perfusion MRI reference standard that showed hemodynamically significant stenoses in 73 (73%) patients with 117 (39%) vessel territories subtended. The diagnostic performance of combined coronary CTA and stress perfusion DECT versus combined ICA and cardiovascular stress perfusion MRI is shown in Table 3. For combined coronary CTA and stress perfusion DECT interpretation, AUC increased to 0.84 from 0.78 ($p = 0.02$) for coronary CTA alone on per-vessel– based analysis in comparison with combined ICA and cardiovascular stress perfusion MRI. The sample size of 300 vessel territories had 80% power in the detection of a difference of 0.06 between coronary CTA with an AUC of 0.78 and the combination of coronary CTA and stress perfusion DECT with an AUC of 0.84 in a two-sided *z*-test at a significance level of 0.05.

Discussion

The main finding of this study is that compared with the reference standard of combined ICA and cardiovascular stress perfusion MRI, stress perfusion DECT has good diagnostic accuracy and incremental diagnostic value over coronary CTA alone in the detection of hemodynamically significant coronary stenosis inducing complete reversible myocardial perfusion defects. Our results help to validate the clinical usefulness of perfusion CT.

Patient outcome in CAD is closely related to revascularization after myocardial perfusion defects induce hemodynamically significant stenosis [25, 26]. FFR has been recognized as the reference standard for determining the functional significance of coronary stenosis, and FFR-guided revascularization strategies have become more widely accepted [27]. SPECT is an established standard for the detection and quantification of myocardial ischemia. Compared with FFR, cardiovascular stress perfusion MRI has excellent diagnostic performance for the discrimination of hemodynamically significant from insignificant stenosis [28] and is an alternative to SPECT in the detection of anatomically significant stenosis with better sensitivity and negative predictive value than ICA [29]. Perfusion CT is an emerging method for imaging of myocardial ischemia and is being investigated with various CT scanners, imaging techniques, study populations, and reference standards. Accordingly, perfusion CT has sensitivity ranging from 50% to 96% and specificity from 51% to 89% for the detection of myocardial perfusion defects according to vessel territory. The combination of coronary CTA and perfusion CT has incrementally increased the value of coronary CTA in the detection of hemodynamically significant coronary stenoses compared with combined ICA and SPECT, combined ICA and cardiovascular stress perfusion MRI, and FFR [10–15].

Considering that cardiovascular stress perfusion MRI has superior spatial resolution to that of SPECT and that the pharmacokinetics of gadolinium-based contrast agents are similar to those of iodine-based CT contrast agents, cardiovascular stress perfusion MRI is more accurate and acceptable than SPECT as the reference standard for perfusion measurement in perfusion CT [30, 31]. Bettencourt et al. [15] directly compared the diagnostic performance of perfusion CT with that of cardiovascular stress perfusion MRI against FFR as the reference standard in the same patients. They found that perfusion CT was globally inferior to cardiovascular stress perfusion MRI for the detection of CAD but that CT protocols integrating coronary CTA and perfusion CT depicted hemodynamically significant CAD and had a diagnostic performance similar to that of cardiovascular stress perfusion MRI.

DECT is a newer imaging technique for mapping myocardial iodine distribution [16–18]. Theoretically, the combined use of DECT and perfusion CT (stress perfusion DECT) has the potential to be superior to conventional perfusion CT for the detection of perfusion defects. Our results do not address that hypothesis because it is beyond the scope of this study. However, stress perfusion DECT results are in line with those in published studies [10–15, 20]. Integration of stress perfusion DECT and coronary CTA improves coronary CTA performance for the detection of hemodynamically significant stenosis as assessed with combined ICA and cardiovascular stress perfusion MRI. The integration increases the specificity from 61% to 79%, positive predictive value from 61% to 73%, AUC from 0.78 to 0.84, and the kappa value from 0.5 to 0.65. However, the pervessel specificity and positive predictive value of stress perfusion DECT were lower than those of single-energy perfusion 64-MDCT (95% and 78%) and dual-source 128-MDCT (95% and 96%) compared with combined cardiovascular stress perfusion MRI and delayed enhancement [12, 15]. This could be justified by differences in the study populations (inclusion vs exclusion of patients with chronic myocardial infarction) and CT scanners with a perfusion protocol (64-MDCT or high-pitch dual-source 128-MDCT with single-energy mode vs dual-source 64-MDCT in dual-energy mode).

Importantly, Feuchtner et al. [12] found that the sensitivity of perfusion CT for detection of complete and partial reversible perfusion defects (68%) was lower than that for fixed perfusion defects (84%). In our study, none of the patients had segments with partial reversible or fixed perfusion defects. Furthermore, our results were largely attributed to the rapid heart rate (84 ± 17 beats/min) and wide heart rate difference (13 ± 14 beats/min) that affect the image quality of stress perfusion DECT. Stress perfusion DECT is prone to cardiac motion artifacts due to the limited temporal resolution of DECT (330 milliseconds) not to overcoming rapid heart rate. The temporal resolution of dual-source CT in dual-energy mode is not sufficient to freeze cardiac motion to a larger extent than single-energy dual-source CT, which is the major cause of degradation of the image quality of DECT-based myocardial iodine maps [19, 20]. In addition, normal nonuniform distribution of iodine within the myocardium and beam-hardening artifacts were misinterpreted as myocardial perfusion defects on iodine maps in stress perfusion DECT [17]. Accordingly, the performance of perfusion DECT in this study would appear to be worse than the published data on the performance of single-energy perfusion CT show.

Limitations

Our study had several limitations. First, in this single-center study, only patients with suspected or known CAD without chronic myocardial infarction detected with coronary CTA were included. Accordingly, 82% of subjects had significant coronary stenoses at ICA, and 75% had perfusion defects at cardiovascular stress perfusion MRI. The prereferral bias might have affected interpretation of both stress perfusion DECT and cardiovascular stress perfusion MR images, leading to rather optimistic test results and limitation in generalization of the test results.

Second, we did not measure the extent and severity of perfusion defects associated with any quantitative parameters but only visually detected perfusion defects on stress perfusion DECT–based iodine maps. Quantitative measurement on stress perfusion DECT images may yield objective criteria for considering myocardial perfusion defects.

Third, the results of our study are applicable only to the specific CT scanner used because the stress perfusion DECT protocol is not feasible with other clinical CT scanners. In addition, we did not compare the diagnostic performance of stress perfusion DECT–based iodine maps with that of gray-scale perfusion CT images based on merged data with 70% of the 140-kV spectrum and 30% of the 80-kV spectrum for detection of perfusion defects. Accordingly, we are not convinced that stress perfusion DECT–based iodine mapping is superior to single-energy standard perfusion CT.

Fourth, in spite of directly comparing stress perfusion DECT and cardiovascular stress perfusion MRI in all patients, we used only three short-axis slices for cardiovascular stress perfusion MRI performed with 1.5-T and 3-T MRI systems. Accordingly, small perfusion defects might have been missed with cardiovascular stress perfusion MRI. Slice-by-slice comparison of cardiovascular stress perfusion MRI with stress perfusion DECT data would be required to determine the real agreement. Our results might have been impaired by the limitations of cardiovascular stress perfusion MRI because false-positive findings are likely.

Fifth, several of the measurements obtained from the imaging studies included operator- and interpreter-dependent steps. We did not, however, evaluate intraobserver variability in perfusion interpretation with DECT and cardiovascular MRI or intraobserver and interobserver agreement regarding coronary CTA interpretation.

Sixth, in clinical practice, coronary CTA and perfusion CT usually are performed together. In the current study, however, the separate time points for coronary CTA and stress perfusion DECT raise the question of the applicability of the findings and diminish the possibility of simultaneous acquisition of anatomic and functional information. The use of separate time points also has the disadvantage that in practical clinical settings, the patient would need to return for a separate examination and a second IV contrast injection.

Seventh, the specificity and positive predictive value of coronary CTA in this study were slightly lower than previously reported for coronary CTA [1, 2]. The degree of stenosis was overestimated with coronary CTA, particularly in patients with high heart rates, which increased the proportion of calcified lesions read as indeterminate or significant. A higher proportion of such lesions would not have been significant or have exhibited perfusion defects with the reference methods but might have been excluded with better heart rate control by use of IV β-blockers in combination with the oral drug used.

Finally, radiation exposure of patients with the applied protocol is still considerable. The mean radiation exposure for the coronary CTA protocol was 7.3 ± 1.7 mSv and for stress perfusion DECT was 4.2 ± 1.1 mSv. We did not obtain rest phase and delayed enhancement phase images after stress perfusion DECT because of the characteristics of the study population undergoing the coronary CTA protocol and previous acquisition with single-energy CT. We used stress perfusion DECT and resting perfusion CT by coronary CTA for the direct comparison with cardiovascular perfusion MRI. This protocol design was justified in light of reducing radiation exposure of patients.

Conclusion

Stress perfusion DECT has the potential to become a robust clinical tool for the detection of myocardial ischemia and can be used as an alternative to other perfusion imaging techniques. The combined approach of coronary CTA and stress perfusion DECT allows identification of hemodynamically significant coronary lesions inducing perfusion defects in CAD patients and thereby provides useful information for assessing the need for combined ICA and cardiovascular stress perfusion MRI or FFR. Importantly, stress perfusion DECT can play a complementary role in enhancing the accuracy of coronary CTA for identifying hemodynamically significant stenosis. However, larger multicenter clinical studies are needed for further investigation of the diagnostic accuracy of stress perfusion DECT.

Acknowledgments

Research reported in this publication was supported by the National Heart, Lung, and Blood Institute of the National Institutes of Health (Bethesda, Maryland) under Award Number R01HL111141.

Supported by Bayer Schering Pharma, Berlin, Germany.

References

1. Vanhoenacker PK, Heijenbrok-Kal MH, Van Heste R, et al. Diagnostic performance of multidetector CT angiography for assessment of coronary artery disease: meta-analysis. Radiology. 2007; 244:419–428. [PubMed: 17641365]
2. Alkadhi H, Scheffel H, Desbiolles L, et al. Dual-source computed tomography coronary angiography: influence of obesity, calcium load, and heart rate on diagnostic accuracy. Eur Heart J. 2008; 29:766–776. [PubMed: 18292596]
3. Sato A, Hiroe M, Tamura M, et al. Quantitative measures of coronary stenosis severity by 64-slice CT angiography and relation to physiologic significance of perfusion in nonobese patients: comparison with stress myocardial perfusion imaging. J Nucl Med. 2008; 49:564–572. [PubMed: 18344444]
4. Gaemperli O, Schepis T, Valenta I, et al. Functionally relevant coronary artery disease: comparison of 64-section CT angiography with myocardial perfusion SPECT. Radiology. 2008; 248:414–423. [PubMed: 18552310]
5. Santana CA, Garcia EV, Faber TL, et al. Diagnostic performance of fusion of myocardial perfusion imaging (MPI) and computed tomography coronary angiography. J Nucl Cardiol. 2009; 16:201–211. [PubMed: 19156478]
6. Gaemperli O, Schepis T, Valenta I, et al. Cardiac image fusion from stand-alone SPECT and CT: clinical experience. J Nucl Med. 2007; 48:696–703. [PubMed: 17475956]
7. Scheffel H, Stolzmann P, Alkadhi H, et al. Low-dose CT and cardiac MR for the diagnosis of coronary artery disease: accuracy of single and combined approaches. Int J Cardiovasc Imaging. 2010; 26:579–590. [PubMed: 20146002]
8. Tamarappoo BK, Dey D, Nakazato R, et al. Comparison of the extent and severity of myocardial perfusion defects measured by CT coronary angiography and SPECT myocardial perfusion imaging. JACC Cardiovasc Imaging. 2010; 3:1010–1019. [PubMed: 20947046]
9. Blankstein R, Shturman LD, Rogers IS, et al. Adenosine-induced stress myocardial perfusion imaging using dual-source cardiac computed tomography. J Am Coll Cardiol. 2009; 54:1072–1084. [PubMed: 19744616]
10. Rocha-Filho JA, Blankstein R, Shturman LD, et al. Incremental value of adenosine-induced stress myocardial perfusion imaging with dual-source CT at cardiac CT angiography. Radiology. 2010; 254:410–419. [PubMed: 20093513]
11. Ko BS, Cameron JD, Meredith IT, et al. Computed tomography stress myocardial perfusion imaging in patients considered for revascularization: a comparison with fractional flow reserve. Eur Heart J. 2012; 33:67–77. [PubMed: 21810860]
12. Feuchtner G, Goetti R, Plass A, et al. Adenosine stress high-pitch 128-slice dual-source myocardial computed tomography perfusion for imaging of reversible myocardial ischemia: comparison with magnetic resonance imaging. Circ Cardiovasc Imaging. 2011; 4:540–549. [PubMed: 21862731]
13. George RT, Arbab-Zadeh A, Miller JM, et al. Adenosine stress 64- and 256-row detector computed tomography angiography and perfusion imaging: a pilot study evaluating the transmural extent of perfusion abnormalities to predict atherosclerosis causing myocardial ischemia. Circ Cardiovasc Imaging. 2009; 2:174–182. [PubMed: 19808590]
14. George RT, Arbab-Zadeh A, Miller JM, et al. Computed tomography myocardial perfusion imaging with 320-row detector computed tomography accurately detects myocardial ischemia in patients with obstructive coronary artery disease. Circ Cardiovasc Imaging. 2012; 5:333–340. [PubMed: 22447807]
15. Bettencourt N, Chiribiri A, Schuster A, et al. Direct comparison of cardiac magnetic resonance and multidetector computed tomography stress-rest perfusion imaging for detection of coronary artery disease. J Am Coll Cardiol. 2013; 61:1099–1107. [PubMed: 23375929]
16. Ruzsics B, Lee H, Zwerner PL, et al. Dual-energy CT of the heart for diagnosing coronary artery stenosis and myocardial ischemia-initial experience. Eur Radiol. 2008; 18:2414–2424. [PubMed: 18523782]
17. Schwarz F, Ruzsics B, Schoepf UJ, et al. Dual-energy CT of the heart–principles and protocols. Eur J Radiol. 2008; 68:423–433. [PubMed: 19008064]

18. Ruzsics B, Schwarz F, Schoepf UJ, et al. Comparison of dual-energy computed tomography of the heart with single photon emission computed tomography for assessment of coronary artery stenosis and of the myocardial blood supply. Am J Cardiol. 2009; 104:318–326. [PubMed: 19616661]
19. Ko SM, Choi JW, Song MG, et al. Myocardial perfusion imaging using adenosine-induced stress dual-energy computed tomography of the heart: comparison with cardiac magnetic resonance imaging and conventional coronary angiography. Eur Radiol. 2011; 21:26–35. [PubMed: 20658242]
20. Ko SM, Choi JW, Hwang HK, et al. Diagnostic performance of combined noninvasive anatomic and functional assessment with dual-source CT and adenosine-induced stress dual-energy CT for detection of significant coronary stenosis. AJR. 2012; 198:512–520. [PubMed: 22357990]
21. Austen WG, Edwards JE, Frye RL, et al. A reporting system on patients evaluated for coronary artery disease. Report of the AD Hoc Committee for Grading of Coronary Artery disease, Council on Cardiovascular Surgery, American Heart Association. Circulation. 1975; 51(suppl):5–40. [PubMed: 1116248]
22. Cerqueira MD, Weissman NJ, Dilsizian V, et al. Standardized myocardial segmentation and nomenclature for tomographic imaging of the heart: a statement for healthcare professionals from the Cardiac Imaging Committee of the Council on Clinical Cardiology of the American Heart Association. Circulation. 2002; 105:539–542. [PubMed: 11815441]
23. Pilz G, Klos M, Ali E, Hoefling B, Scheck R, Bernhardt P. Angiographic correlations of patients with small vessel disease diagnosed by adenosine-stress cardiac magnetic resonance imaging. J Cardiovasc Magn Reson. 2008; 10:8. [PubMed: 18275591]
24. Hausleiter J, Meyer T, Hermann F, et al. Estimated radiation dose associated with cardiac CT angiography. JAMA. 2009; 301:500–507. [PubMed: 19190314]
25. Shaw LJ, Berman DS, Maron DJ, et al. Optimal medical therapy with or without percutaneous coronary intervention to reduce ischemic burden: results from the Clinical Outcomes Utilizing Revascularization and Aggressive Drug Evaluation (COURAGE) trial nuclear substudy. Circulation. 2008; 117:1283–1291. [PubMed: 18268144]
26. Tonino PA, De Bruyne B, Pijls NH, et al. Fractional flow reserve versus angiography for guiding percutaneous coronary intervention. N Engl J Med. 2009; 360:213–224. [PubMed: 19144937]
27. Wijns W, Kolh P, Danchin N, et al. Guidelines on myocardial revascularization. Eur Heart J. 2010; 31:2501–2555. [PubMed: 20802248]
28. Watkins S, McGeoch R, Lyne J, et al. Validation of magnetic resonance myocardial perfusion imaging with fractional flow reserve for the detection of significant coronary heart disease. Circulation. 2009; 120:2207–2213. [PubMed: 19917885]
29. Greenwood JP, Maredia N, Younger JF, et al. Cardiovascular magnetic resonance and single-photon emission computed tomography for diagnosis of coronary heart disease (CE-MARC): a prospective trial. Lancet. 2012; 379:453–460. [PubMed: 22196944]
30. Nandalur KR, Dwamena BA, Choudhri AF, et al. Diagnostic performance of stress cardiac magnetic resonance imaging in the detection of coronary artery disease: a meta-analysis. J Am Coll Cardiol. 2007; 50:1343–1353. [PubMed: 17903634]

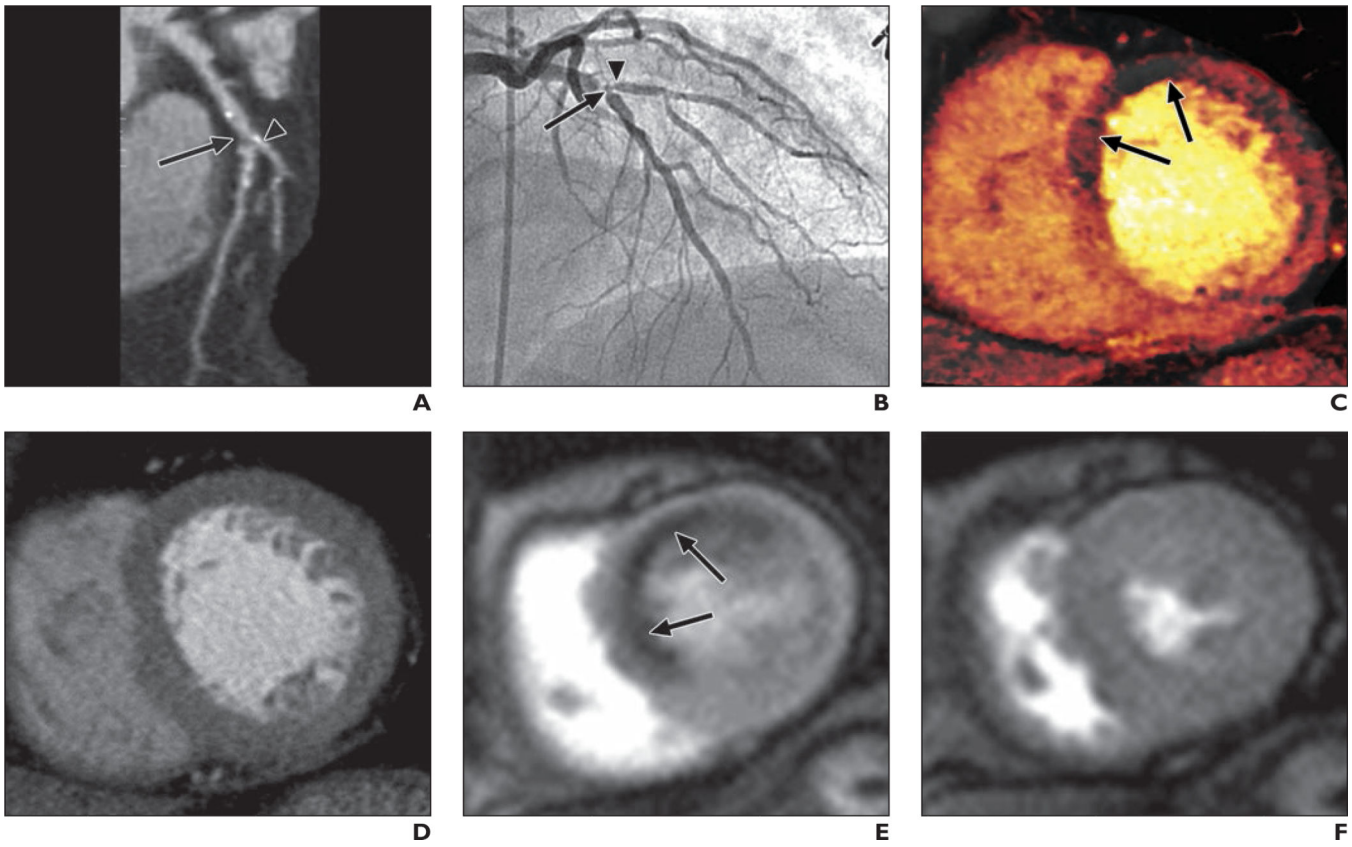

Fig. 1. 63-year-old woman with severe chest pain on exercise

A, Curved multiplanar reformatted coronary CT angiogram shows ostial calcification with second diagonal branch (*arrowhead*) and significant stenosis with noncalcified plaque (*arrow*) in midsegment of left anterior descending coronary artery (LAD).

B, Invasive coronary angiogram confirms presence of significant bifurcation stenosis involving mid LAD (*arrow*) and ostium of second diagonal branch (*arrowhead*).

C, Dual-energy CT iodine map obtained during adenosine infusion shows blood-pool defects (*arrows*) in mid anteroseptal and anterior left ventricular myocardium.

D, Rest perfusion CT image does not show any perfusion defects in left ventricular myocardium.

E and **F,** Cardiovascular MR images acquired at stress (**E**) and rest (**F**) show complete reversible subendocardial perfusion defects (*arrows*, **E**) in mid anteroseptal and anterior left ventricular myocardium.

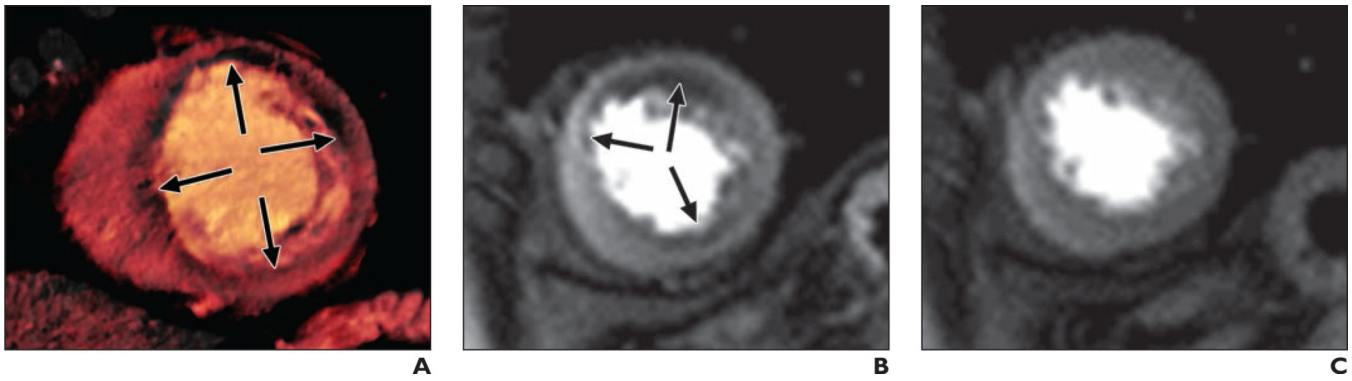

Fig. 2. 70-year-old woman with chest pain on exercise and with dyspnea

A, Dual-energy CT iodine distribution map obtained during adenosine infusion shows blood-pool defects (*arrows*) in mid anterior and anterolateral and inferior left ventricular myocardium.

B and **C,** Cardiovascular MR images acquired at stress (**B**) and rest (**C**) show reversible subendocardial perfusion defects (*arrows*, **B**) in mid anterior, septal and inferior left ventricular myocardium. There was no delayed hyperenhancement in left ventricular myocardium at delayed contrast-enhanced cardiovascular MRI (not shown).

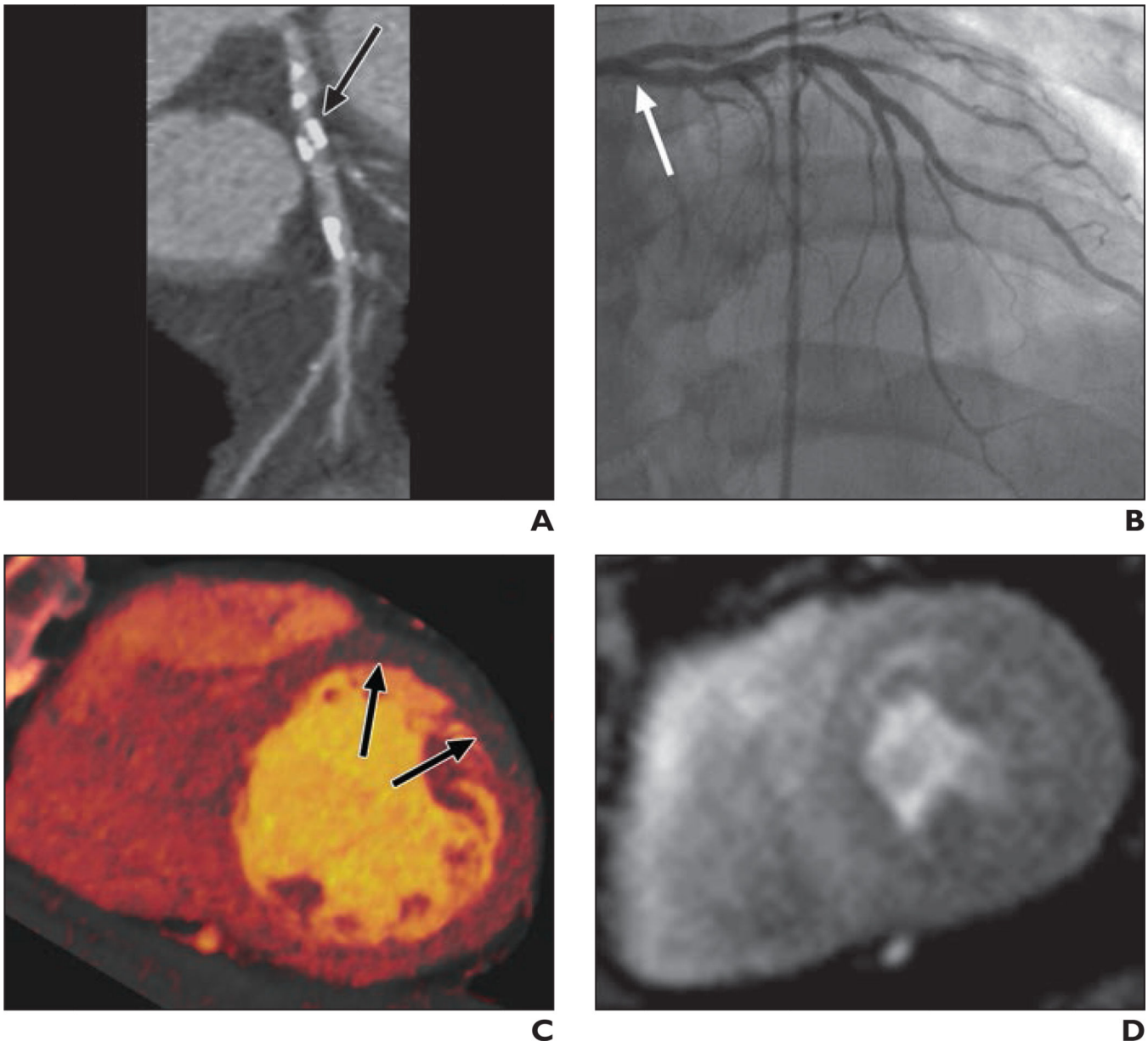

Fig. 3. 61-year-old man with chronic chest pain and bicuspid aortic valve disease

A, Curved multiplanar reformatted coronary CT angiogram shows heavily calcified plaque (*arrow*) in proximal segment of left anterior descending coronary artery (LAD).

B, Invasive coronary angiogram confirms insignificant stenoses (*arrow*) in proximal LAD.

C, Dual-energy CT iodine distribution map obtained during adenosine infusion shows blood-pool defects (*arrows*) in mid anterior left ventricular myocardium.

D, Cardiovascular MR image acquired at stress shows no perfusion defects in mid left ventricular myocardium.

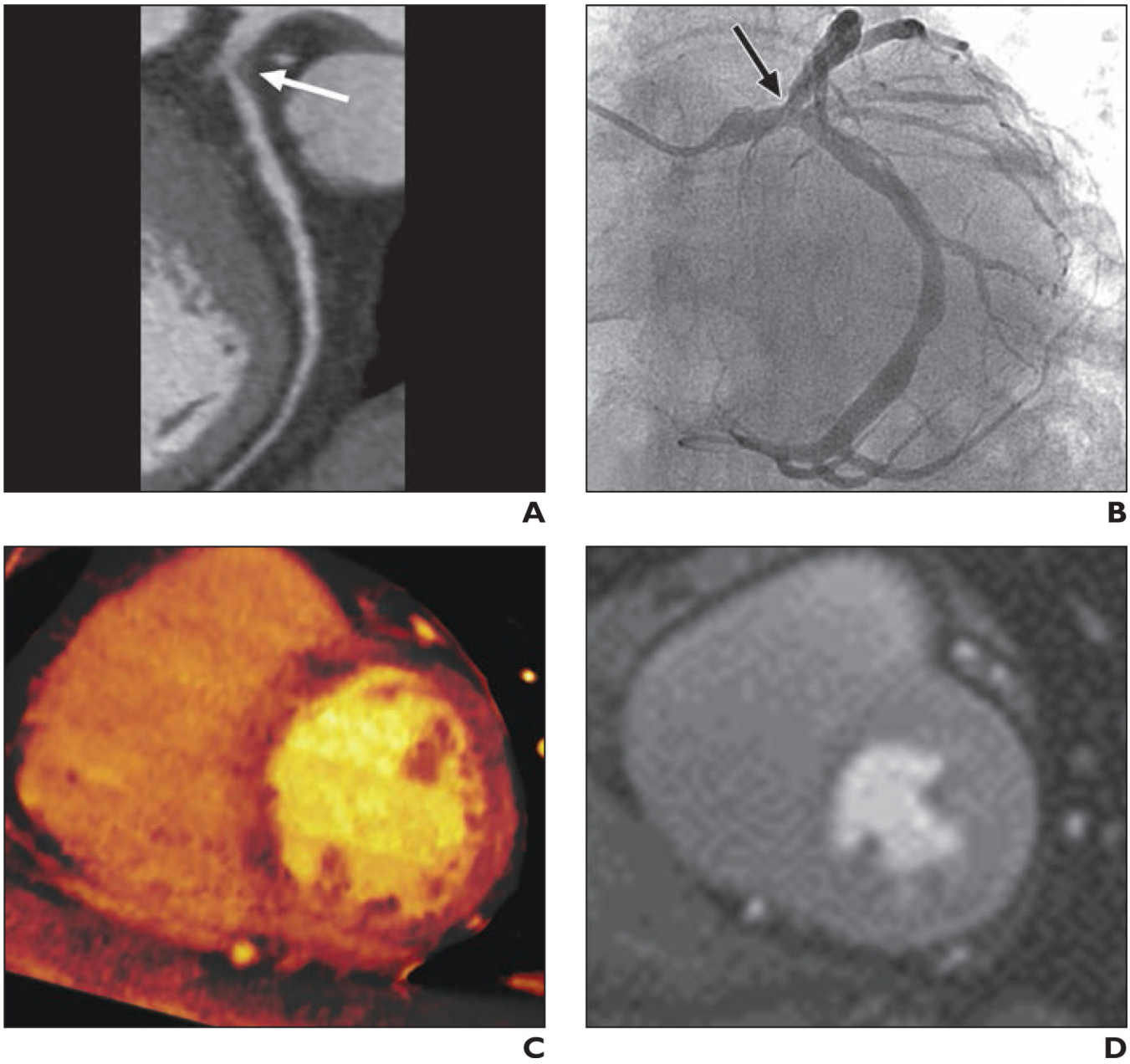

Fig. 4. 68-year-old man with chronic chest pain and atherosclerotic abdominal aortic aneurysm

A, Curved multiplanar reformatted coronary CT angiogram shows significant stenosis with noncalcified plaque (*arrow*) in ostium of left anterior descending coronary artery (LAD).

B, Invasive coronary angiogram confirms insignificant stenosis (*arrow*) in ostium of LAD.

C, Dual-energy CT iodine map obtained during adenosine infusion shows no perfusion defects in left ventricular myocardium.

D, Cardiovascular MR image obtained at stress shows no perfusion defects in left ventricular myocardium.

TABLE 1

Clinical Characteristics of Patient Population (*n* = 100)

Characteristic	Value
Mean age (y)	62.7 ± 8.2
Sex (no.)	
Men	67
Women	33
Body mass index	25.9 ± 2.8
Risk factors	
Smoking history	46
Hypertension	67
Diabetes mellitus	28
Hyperlipidemia	53
Obesity	9
Medical history	
Previous angina	42
Previous myocardial infarction	0
Peripheral vascular disease	3
Previous cerebrovascular accident	6
Previous coronary revascularization	4
Baseline medication	
Aspirin	52
β-Blocker	59
Statin	29

Note—Values are number of patients or mean ± SD.

TABLE 2

Diagnostic Accuracy of Stress Perfusion Dual-Energy CT Compared With Cardiovascular Stress Perfusion MRI for Detection of Reversible Myocardial Perfusion Defects

Diagnostic Performance Measure	Per Segment	Per Vessel	Per Patient
True-positive (no.)	365	116	73
False-positive (no.)	211	44	16
True-negative (no.)	863	126	9
False-negative (no.)	114	14	2
Sensitivity (%)	76 (72–80)	89 (83–94)	97 (91–100)
Specificity (%)	80 (78–83)	74 (67–81)	36 (18–57)
Positive predictive value (%)	63 (59–67)	73 (65–79)	82 (72–89)
Negative predictive value (%)	88 (86–90)	90 (84–94)	82 (48–98)
Accuracy (%)	79 (77–81)	81 (76–85)	82 (73–89)
κ	0.54 (0.49–0.58)	0.62 (0.53–0.70)	0.41 (0.20–0.62)
AUC	0.78 (0.76–0.80)	0.82 (0.77–0.86)	0.67 (0.57–0.76)

Note—Values in parentheses are 95% CI.

TABLE 3

Diagnostic Accuracy Per Vessel Territory

Diagnostic Performance Measure	Coronary CTA Finding of ≥ 50% Stenosis	Stress Perfusion DECT Finding of Myocardial Perfusion Defect	Coronary CTA Finding of ≥ 50% Stenosis and Stress Perfusion DECT Finding of Myocardial Perfusion Defect
True-positive (no.)	111	108	103
False-positive (no.)	72	52	38
True-negative (no.)	111	131	145
False-negative (no.)	6	9	14
Sensitivity (%)	95 (89–98)	92 (86–96)	88 (81–93)
Specificity (%)	61 (53–68)	72 (64–78)	79 (73–85)
Positive predictive value (%)	61 (53–68)	68 (60–75)	73 (65–80)
Negative predictive value (%)	95 (89–98)	94 (88–97)	91 (86–95)
Accuracy (%)	74 (69–79)	80 (75–84)	83 (78–87)
κ	0.50 (0.42–0.59)	0.60 (0.51–0.69)	0.65 (0.56–0.73)
AUC	0.78 (0.73–0.82)	0.82 (0.77–0.86)	0.84 (0.79–0.88)

Note—Values in parentheses are 95% CI. CTA = CT angiography, DECT = dual-energy CT.